scientific reports

Check for updates

OPEN

Astragaloside IV protects brain cells from ischemia-reperfusion injury by inhibiting ryanodine receptor expression and reducing the expression of P-Src and P-GRK2

Juan Chen[1,4,5], Jun Bao[1,5], Xiujuan Jiang[1], Wentao Yu[1], Yunpeng Han[1], Xia Zhang[1], Ying Zhang[2,3]✉ & Guoxing Deng[1]✉

Astragaloside IV, a prime active component of *Astragalus membranaceus*, has potential as a neuroprotectant. We aimed to identify the active ingredients in *A. membranaceus* and assess if Astragaloside IV can improve cerebral ischemia-reperfusion injury (CIRI) cell apoptosis by reducing P-Src and P-GRK2 via ryanodine receptor (RyR) expression inhibition. We used bioinformatics analysis to examine the effects of *A. membranaceus* on ischemic stroke. We studied brain samples from middle cerebral artery occlusion (MCAO) mice treated with normal saline, Astragaloside IV, and sham mice for pathology and Western blot tests. We also tested PC12 cells *in vitro* with or without Astragaloside IV or GSK180736A using Western blotting and fluorescence assays. Our bioinformatics analysis suggested a possible association between *A. membranaceus*, calcium ion pathways, and apoptosis pathways. Western blot data indicated Astragaloside IV significantly decreased RyR, p-Src, and downstream phosphorylated GRK2, PLC, CaMKII, and IP3R levels in MCAO mice brains. Astragaloside IV also considerably inhibited pro-apoptotic and oxidative stress-associated proteins' expression while boosting anti-apoptotic protein expression. The results suggest Astragaloside IV can inhibit RyR expression, subsequently reducing brain cell apoptosis.

Stroke is the second leading cause of death and a major contributor to disability worldwide. Ischemic stroke is particularly common, accounting for approximately 87% of all stroke types[1,2]. This type of stroke is primarily due to a sudden interruption of blood supply to the brain. Symptoms can include sudden fainting, unconsciousness, speech and cognitive difficulties, and hemiplegia[3]. Although recombinant tissue plasminogen activator (rt-PA) recanalization is an effective method for treating cerebral ischemia, it requires a strict treatment window[4,5]. Moreover, the restoration of blood flow can further aggravate damage to the ischemic brain tissue, a phenomenon known as cerebral ischemia-reperfusion injury (CIRI)[6]. CIRI involves a multitude of complex pathophysiological mechanisms, such as an inflammatory response, oxidative stress, intracellular calcium overload, increased neuronal apoptosis, excessive ion channel opening, and an overabundance of excitatory neurotransmitters[7,8]. Therefore, existing treatment strategies are limited, underscoring an urgent need to develop new therapeutic strategies for preventing CIRI.

In the case of ischemic brain injury, brain cells are subjected to a state of hypoxia and hypoglycemia. Stimulation from hypoxia and hypoglycemia can trigger inflammation, oxidative stress, calcium overload, and apoptosis of brain cells[9]. Research has suggested that inhibiting apoptosis can mitigate the degree of ischemic brain injury and protect brain tissue[5,10–12]. The Src kinase family, comprising of proteins with tyrosine protein kinase activity[13], is structured from the N-terminal to the C-terminal as follows: the SH4 domain, specific fragment, SH3 domain,

[1]College of Basic Medicine, Hebei University of Chinese Medicine, No.3 Xingyuan Road, Shijiazhuang 050200, Hebei, China. [2]College of Nursing, Hebei University of Chinese Medicine, No.3 Xingyuan Road, Shijiazhuang 050200, Hebei, China. [3]Hebei Key Laboratory of Health Care with Traditional Chinese Medicine, Shijiazhuang 050200, Hebei, China. [4]Shenzhen Hospital of Guangzhou University of Chinese Medicine, Shenzhen 518034, Guangdong, China. [5]These authors contributed equally to this work: Juan Chen and Jun Bao. ✉email: yingzhang@hebcm.edu.cn; dengguoxing@hebcm.edu.cn

SH2 domain, ligand segment, SH1 domain, and the carboxy-terminal regulatory tail[14]. One study reported an association between the activity of Src kinase and brain injury post cerebral ischemia[15].

Mitochondria hold a significant role in maintaining the intracellular function of the central nervous system (CNS)[16]. It has been found through studies that intracellular Ca^{2+} release is primarily facilitated by the inositol 1,4,5-trisphosphate receptor (IP3R) and the ryanodine receptor (RyR) on the sarcoplasmic reticulum membrane. Further, the increase of mitochondrial calcium can be induced by the RyR in the endoplasmic reticulum[17,18]. Nonetheless, hypoxic-ischemic brain damage is characterized by a disorder in calcium homeostasis, ultimately leading to neurodegeneration. Therefore, RyR is implicated in the calcium imbalance during and after hypoxia-ischemia[19].

G protein-coupled receptor kinases (GRKs) relate to the rapid desensitization of G protein-coupled receptors (GPCRs). GRK2, which is widely distributed, phosphorylates the β2 adrenergic receptor (β2AR) activated by agonists[20]. The rapid phosphorylation of GRK2 can reduce its interaction with G proteins (Gβγ and Gα) and the ensuing release of Gβγ ultimately leads to phospholipase Cγ (PLCγ) activation. Upon PLCγ activation, inositol (1,4,5) triphosphate (IP3) is produced, which in turn activates IP3 receptors (IP3Rs) and facilitates a continuous Ca^{2+} release via the endoplasmic reticulum[21]. Previous studies have indicated that Ca^{2+} release mediated by IP3R plays an influential role in regulating cytosolic and nuclear Ca^{2+} signals[22]. Furthermore, studies suggest that reperfusion can enhance intracellular Ca^{2+} release and activate the Ca^{2+}/CaM-dependent protein kinase II (CaMKII)[23,24].

Astragalus membranaceus was first documented in the *Shennong Bencao Jing*, which is China's earliest complete pharmacopeia. It is renowned for its diverse therapeutic effects[25,26]. For instance, *A. membranaceus* is a key ingredient in Buyang Huanwu Decoction, a treatment documented in "Yilin Gaicuo", a book from the Qing Dynasty authored by Wang Qingren. This treatment has been extensively applied in managing ischemic stroke, exhibiting significant neuroprotective effects[27,28]. *A. membranaceus* primarily consists of three types of chemical compounds: polysaccharides, saponins, and flavonoids, with Astragaloside IV being one of its primary active components[29]. Among its many properties, Astragaloside IV is noted for scavenging oxygen free radicals, providing anti-inflammatory and anti-viral effects, improving bodily immunity, and enhancing cardiovascular function[30]. This compound is also recognized for reducing the activity of myeloperoxidase, thereby mitigating inflammation in a rat model of cerebral ischemia-reperfusion[31]. Our preliminary research indicates that Astragaloside IV can also diminish CIRI in rats[32]. Following treatment with Astragaloside IV, PC12 cells displayed a considerable decline in the apoptosis rate and index[33]. However, the mechanisms of action between Astragaloside IV, p-Src, and p-GRK2, as well as the role Astragaloside IV plays in treating CIRI, remain unknown at present.

Medical bioinformatics is an interdisciplinary field that employs computer science to store, retrieve, analyze, and interpret biological and medical data. In recent years, the rapid advancement of gene chips and high-throughput sequencing technology has facilitated comprehensive analysis of the transcriptome and genome. This has been instrumental in the progression and development of the life sciences. With the escalation of related studies on gene expression profiles of CIRI and the establishment of various public databases, it is now feasible to conduct in-depth research on CIRI using bioinformatics methods. This has extended our understanding of the pathological mechanism of CIRI[34].

Therefore, this study aims to utilize bioinformatics technology to investigate the core genes associated with ischemic stroke and perform enrichment analysis and pathway analysis. The cause of CIRI is not clearly understood, making it crucial to clarify its pathogenesis for timely and effective treatment. Hence, in this study, we further examine the pathogenesis of CIRI by observing oxidative stress-related proteins (P22, P47, GP91)[35], apoptosis-related proteins (caspase-3, caspase-8, caspase-9, Bax, Bcl-2)[36], and mitochondrial calcium overload-related proteins (p-GRK2, p-PLCβ, p-PLCA, p-CaMKII, p-IP3R, RyR)[23]. A common dataset was utilized to substantiate the significant role of p-Src and p-GRK2 in CIRI, confirmed through a basic cell experiment.

Materials and methods

Ethical approval

The Ethics Committee of the Hebei University of Chinese Medicine approved all experimental protocols. The research was conducted following all relevant guidelines and regulations of the Ethics Committee of Hebei University of Chinese Medicine (DWLL2020080). We reported all methods in accordance with ARRIVE guidelines.

Data acquisition

Research lab materials consist of the database and analysis software, the pharmacology database system of Traditional Chinese Medicine (TCM), which includes a database and analysis platform TCMSP (http://tcmspw.com/tcmsp.php), as well as the Human Genome database (https://www.genecards.org/). Other resources include the Protein Target database Uniprot (https://www.uniprot.org/), the Gene Expression Omnibus (GEO) database (https://www.ncbi.nlm.nih.gov/geo/), and the signaling pathway analysis database, DAVID (https://david.ncifcrf.gov/). The utilized analysis software features include Cytoscape 3.8.2 and the CytoHubba plugin.

Screening the active constituents of *A. membranaceus*

Using the TCMSP database (http://tcmspw.com/tcmsp.php), we queried the chemical composition of *A. membranaceus*, adopting the screening functions for oral bioavailability (OB) values and drug-likeness (DL) scores (with a threshold of OB 30% and DL 0.18 or above), and identify potential active compounds. Thus, the target active ingredients of *A. membranaceus* were deduced by this screening procedure.

Screening for active ingredient targets and the construction of a component-target network

The corresponding targets of *A. membranaceus*, acquired from TCMSP, were used to query relative genes in GeneCards and UniProt databases. After weight reduction, the corresponding gene targets of the target components were obtained. The component targets were then imported into Cytoscape 3.8.2, and a "component-target" network regarding *A. membranaceus* was established using the CytoHubba plugin. Network Analyzer was used to assess the centrality of network nodes, selecting the Degree value as the screening condition. The higher the Degree value, the component is related to more targets, aiding the analysis of core compounds and core action targets.

Prediction of *A. membranaceus* and disease targets and GO and KEGG enrichment analysis

Data sets related to ischemic stroke were downloaded from the GEO database. The standardization and gene analysis of quantile RNA seq data were conducted using the R language limma package, considering P value < 0.05 and | logFC | > 1. The identified targets that are related to the active components of *A. membranaceus* and ischemic stroke were imported into the Wayne tool for interaction analysis. This process yielded a target intersection. The selected DEGs were imported into the DAVID database, with all target gene names corrected to their official gene symbol by defining the species as human and inputting the target gene name list. A threshold P value < 0.05 was set using the above database's retrieval and transformation operation. Gene Ontology (GO) biological process enrichment analysis and Kyoto Encyclopedia of Genes and Genomes (KEGG) signal pathway enrichment analysis were then executed, and their results were depicted in the form of advanced bubble graphs using R language.

Gene set enrichment analysis (GSEA)

The Gene Set Enrichment Analysis (GSEA) tool (http://www.gsea-msigdb.org/) was utilized for the analysis of all genes. The pathway for GSEA enrichment was subsequently mapped.

Animal experiments

A total of 32 Specific Pathogen Free (SPF) male C57BL/6J mice, each weighing 30 g and aged 8 weeks, were used in this experiment. Mice were purchased from the Beijing Charles River Company. The mice were housed in ventilated cages, located in a laboratory with controlled conditions: the temperature was maintained at 25℃, the humidity at 55%, and the light/dark cycle managed at a 12h:12h ratio. We did not restrict their access to either water or food.

Middle cerebral artery occlusion model

A model of middle cerebral artery occlusion (MCAO) was established. Adult C57BL/6J mice were subjected to deep anesthesia with 0.5% pentobarbital sodium. A midline neck incision was made and then pulled apart. Under a microscope, the incision revealed the common carotid arteries, external carotid arteries (ECA), and internal carotid arteries (ICA). A 6+0 nylon monofilament coated with silicone rubber (Doccol) was introduced into the left internal carotid artery through the stump of the external carotid to block the origin of the MCAO and prevent blood flow to the striatum and cortex. After 60 min, reperfusion was initiated via withdrawal of the wire and the incision was sutured. Once the mice regained consciousness, their sensorimotor deficits were evaluated by a blinded observer using the Zea Longa 5-point neurological scoring system[37]. The scoring is as follows: 0 point, normal performance with no neurological deficits; 1 point, failure to fully extend contralateral front paws; 2 points, a tendency to circle to the opposite side; 3 points, falling to the opposite side while walking; or 4 points, no spontaneous walking, and loss of consciousness. Mice scoring between 1 and 3 were selected as experimental subjects. The body temperature was maintained at 37 ± 0.5°C throughout the entire process. No animals perished during the MCAO procedure.

Treatment and sampling

Astragaloside IV was supplied by Chengdu Diao Jiuhong Pharmaceutical Co., LTD. Following our earlier study, Astragaloside IV was injected intraperitoneally at 20 mg/kg for 25 days[28]. On the 26th day, the mice were anesthetized using 0.5% pentobarbital sodium. The hippocampal tissues and cerebral cortex of the mice were subject to TUNEL staining and Western blot analysis.

TUNEL staining

The cerebral cortex was thoroughly fixed in a 40 g/L paraformaldehyde solution for 48 h, dehydrated, embedded in paraffin, sectioned, and then stained with TUNEL (C1088, Beyotime). The sections were subsequently dewaxed, dehydrated, and washed with PBS three times, with each wash lasting 5 min. Following this, the sections were incubated with Protease K (20 μg/mL) for 15 min, and then washed. TUNEL reaction solution (50 μL) was then added to the samples, and the negative control was treated with 50 μL of labeled solution and incubated at 37 ℃ for 60 min in light-protected conditions. After washing, the plate was sealed with an anti-fluorescence quenching agent containing DAPI. Under a fluorescence microscope, apoptotic cells were observed.

Western Blotting

The tissue was ground evenly, and RIPA protein lysate was utilized to extract the total protein from brain tissue on ice. The protein concentration was measured using the Bradford method. After 5% SDS-PAGE electrophoresis, mold transfer, and skim milk powder closure, the primary antibody was added and incubated overnight at 4 ℃ on a shaking table. The corresponding secondary antibody, diluted in the appropriate proportion, was

added and left to incubate at room temperature for 60 min. The ECL chemiluminescence method was deployed for darkroom exposure development. The film was scanned, archived, and organized in PhotoShop to remove color. This independent experiment was repeated thrice, and the average value was recorded.

Oxidative stress detection
To evaluate the effect of Astragaloside IV on oxidative stress, we examined the expression of reactive oxygen species (ROS), superoxide dismutase (SOD), and malondialdehyde (MDA) levels in brain tissues and PC12 cells, following the instructions of the kits.

Cell experiments

Cell culture
PC12 cells were procured from the Kunming Institute of Zoology, Chinese Academy of Sciences (Kunming, China), and maintained in RPMI 1640 medium. This medium was supplemented with 10% fetal bovine serum (FBS), 100 U/mL penicillin, and 100μg/ mL streptomycin. The cells were stored at 37 °C under humid conditions with a composition of 5% CO_2 and 95% air.

Oxygen glucose deprivation-reperfusion (OGD/R) was performed on PC12 cells as previously reported[38]. These cells, during the logarithmic growth phase and in good health, were cultured in serum/glucose-free medium at 37 °C under an atmosphere with 95% N_2 and 5% CO_2 for 2 h. The cultures were then returned to their original conditions and kept in an atmosphere with 95% air and 5% CO_2. In the inhibitor assay, influenced by our previous study, cells were pre-cultured with 20 μg/mL of GSK180736A (HY-18990, MedChemExpress) for 3 h before incubation. They were then cultured with 100 μM of Astragaloside IV for 24 h[32]. It is worth noting that GSK180736A is a GRK2 selective inhibitor and a Rho-associated coiled-coil-containing protein kinase inhibitor[39,40].

Immunofluorescence
The cell slides were fixed with 4% paraformaldehyde for 20 min and then washed three times with PBS. We added a peroxidase blocker and incubated the slide for 30 min. After cleaning, non-immune animal serum was introduced for 120 min. We then added the primary antibody and left it to incubate overnight at 4 ℃. Following this, the slides were washed again and a biotin-labeled secondary antibody was added for 60 min. DAPI was then applied and the slide was incubated in the dark for 5 min. The sample was stained using the nucleation technique, and PBST was applied for 5 min. Excess DAPI was washed off four times before sealing the slides with an anti-fluorescence quenching agent.

Cell counting kit (CCK)-8 assay
To assess cell viability, cell proliferation was evaluated utilizing the CCK-8 kit, adhering to the manufacturer's guidelines. PC12 cells were distributed in 96-well plates, and then incubated overnight at 37 °C in a 5% CO_2 incubator. Later, the cells were incubated in a medium infused with 10μL CCK-8 solution for an additional 2 h. Subsequently, the optical density was measured at 450 nm through an enzyme marker instrument.

Cell apoptosis
PC12 cells were seeded at a density of 5×10^5 per well in 6-well cell culture plates and incubated overnight at 37°C in a 5% CO_2 incubator. This was followed by Oxygen Glucose Deprivation-Reperfusion (OGD/R) treatment for 2 h (hypoxia) and 24 h (reoxygenation). After 12 h of reoxygenation, 100 mM astragaloside was administered for an additional 12 h. Cell apoptosis levels were then assessed according to the instructions of the AnnexinV-FITC/PI apoptosis detection kit. The rate of apoptosis was determined using flow cytometry.

Statistical analysis

In this study, all experiments were repeated a minimum of three times to acquire average results. The data are represented as means ± standard error of the mean (SEM). GraphPad Prism 6, a system analysis software, was utilized for all statistical analyses. An unpaired, two-tailed Student's t-test was conducted for the statistical analysis with a P value < 0.05 being regarded as statistically significant.

Results

The active components of *A. membranaceus* were obtained

A search for *A. membranaceus* was conducted in the TCMSP database to obtain the chemical components related to *A. membranaceus*. According to OB ≥ 30% and DL ≥ 0.18, 20 active components were screened (Table 1).

Screening of active ingredient target and construction of component-target network

The active ingredients of *A. membranaceus* were studied using the GeneCards and UniProt databases, with a particular focus on the Homo sapiens species. This resulted in the identification of 202 target genes. The effective components of *A. membranaceus*, along with their interaction targets, were then incorporated into Cytoscape 3.8.2. An interaction network was subsequently constructed, which consisted of 202 targets and 17 compounds (Fig. 1A).

Screening and enrichment analysis of differentially expressed genes in diseases

The ischemic stroke-related dataset GSE22255 was downloaded from the GEO database, and quantile standardization was performed on the data (Fig. 1B, C). Following the GSE22255 screening criteria of P value < 0.05

Serial number	Compound
MOL000033	(3S,8S,9S,10R,13R,14S,17R)-10,13-dimethyl-17-[(2R,5S)-5-pro pan-2-yloctan-2-yl]-2,3,4,7,8,9,11,12,14,15,16,17-dodecahydro-1
	H-cyclopenta[a]phenanthren-3-ol
MOL000098	Quercetin
MOL000211	Mairin
MOL000239	Jaranol
MOL000296	Hederagenin
MOL000354	Isorhamnetin
MOL000371	3,9-di-O-methylnissolin
MOL000374	5'-hydroxyiso-muronulatol-2',5'-di-O-glucoside
MOL000378	7-O-methylisomucronulatol
MOL000379	9,10-dimethoxypterocarpan-3-O-β-D-glucoside
MOL000380	(6aR,11aR)-9,10-dimethoxy-6a,11a-dihydro-6H-benzofurano[3,2-c]chromen-3-ol
MOL000387	Bifendate
MOL000392	Formononetin
MOL000398	Isoflavanone
MOL000417	Calycosin
MOL000422	Kaempferol
MOL000433	FA
MOL000438	(3R)-3-(2-hydroxy-3,4-dimethoxyphenyl)chroman-7-ol
MOL000439	Isomucronulatol-7,2'-di-O-glucosiole
MOL000442	1,7-Dihydroxy-3,9-dimethoxy pterocarpene

Table 1. The active components of *Astragalus membranaceus*

and |logFC| > 1, we identified 287 differentially expressed genes (DEGs) in the mRNA transcript of an ischemic stroke—135 were increased, and 152 were reduced. The ggplot2 software package was used to create a visual grouping DEGs volcano plot of the GSE22255 dataset in R software (Fig. 1D), while the pheatmap package in R was used to draw the cluster analysis heatmap of the DEGs (Fig. 1E).

The Wayne tool was utilized to calculate the disease differential genes and the active ingredient targets of *A. membranaceus*, resulting in the identification of common genes (Fig. 1F). The common DEGs were analyzed by GO and KEGG enrichment analyses. The DAVID online database tool (https://david.ncifcrf.gov/) was employed to analyze the level of biological processes for DEGs by integrating the GO term, and network, and identifying the differentially expressed genes of a biological process. R language was leveraged to illustrate the GO pathway up-regulated pathway diagram (Fig. 1G) and pathway diagram (Fig. 1H) of DEGs. The analysis results indicated enrichment in signal transduction, positive regulation of apoptosis, and innate immune response. Differential genes were used to analyze the KEGG pathway and map out the KEGG pathway diagram (Fig. 1I). The KEGG pathway diagram suggested enrichment in the calcium ion pathway, mineral absorption pathway, DNA replication pathways, and apoptosis pathway.

Gene set enrichment analysis (GSEA)

The GSEA tool (http://www.gsea-msigdb.org/) was utilized for the gene enrichment analysis of all genes, and the GSEA Enrichment Analysis pathway map was constructed. The results demonstrated that the apoptosis and calcium ion signaling pathways were notably enriched (Fig. 1J–K).

Astragaloside IV inhibited CIRI-induced apoptosis in the hippocampus and cerebral cortex

TUNEL staining was utilized to determine the apoptotic index of the hippocampus and cerebral cortex 7 days after 2 h of MCAO. The representations of TUNEL staining in the infarct area from the four groups are shown (magnification: 40×; scale bar: 50 μm) (Fig. 2A). A histogram illustrated the number of TUNEL-positive cells in the various groups. The number of apoptotic cells in the hippocampus and cerebral cortex saw a significant decrease in the MCAO+Astragaloside IV group compared to the MCAO group (Fig. 2B).

Astragaloside IV inhibited the expression of RyR and p-Src in the MCAO mice model

The protein levels of RyR and p-Src were detected by Western blot. Representative blots and bar graphs from four groups are presented, with GAPDH used as a loading control. Relative protein expression levels of RyR and p-Src were normalized to that of GAPDH. The Western blot assay revealed that Astragaloside IV significantly decreased the expression levels of RyR and p-Src in the brains of MCAO mice (Fig. 3).

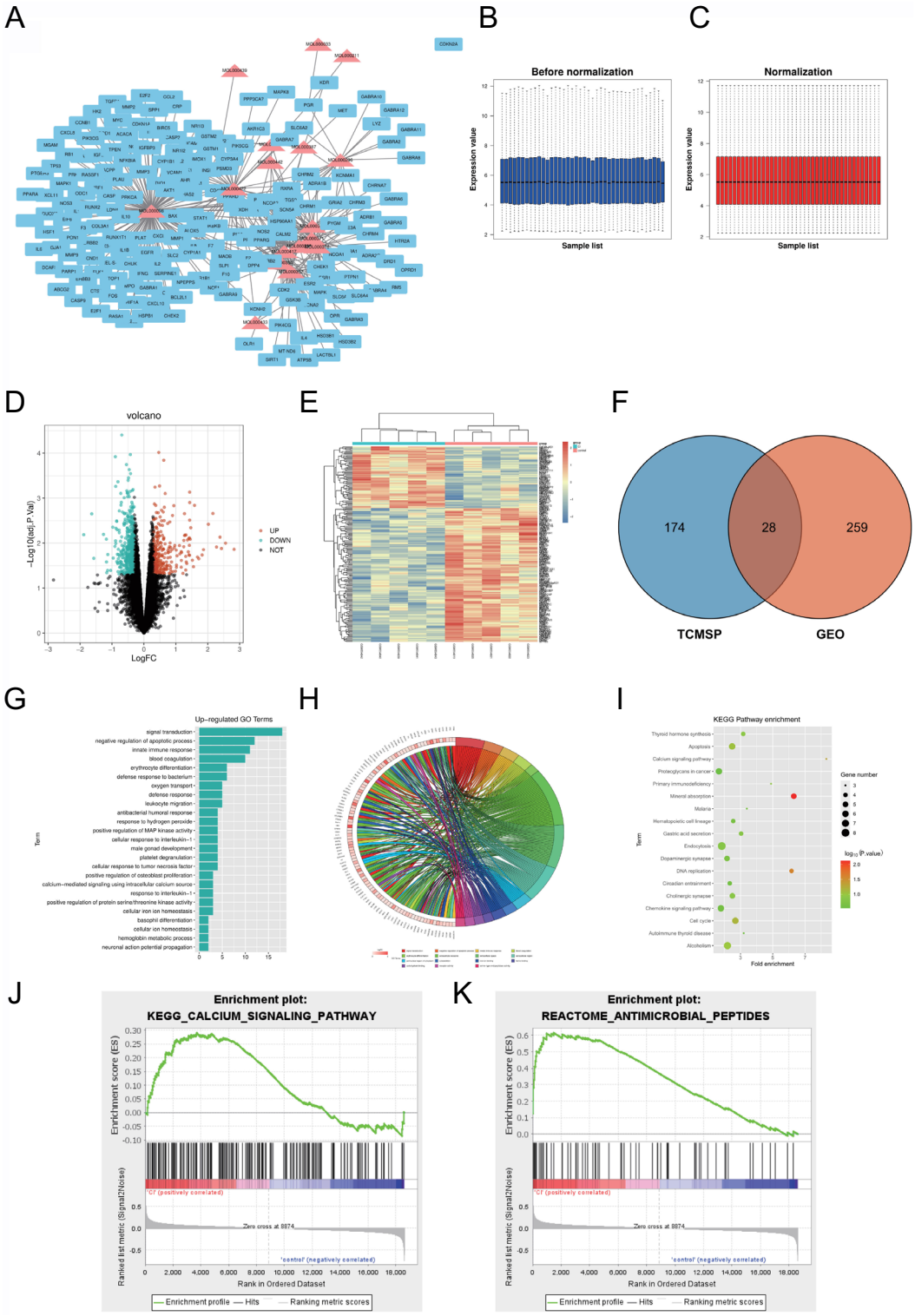

Figure. 1. Bioinformatics analysis of the functional role of *Astragalus membranaceus* on ischemic stroke. **A** Active components of *A. membranaceus* and their interaction target maps. **B** Before normalization. **C** Normalization. **D** Visual Grouping DEGs Volcano Maps. **E** Heatmap of DEGs clustering analysis. **F** Disease-differentiating genes and active ingredient targets in *A. membranaceus*. **G** GO pathway up-regulation pathway map of DEGs. **H** GO pathway up-regulation pathway map of DEGs. **I** The KEGG pathway was analyzed using differential genes and a KEGG pathway map was drawn. **J** Calcium ion signaling pathways were enriched. **K** Apoptosis signaling pathways were enriched.

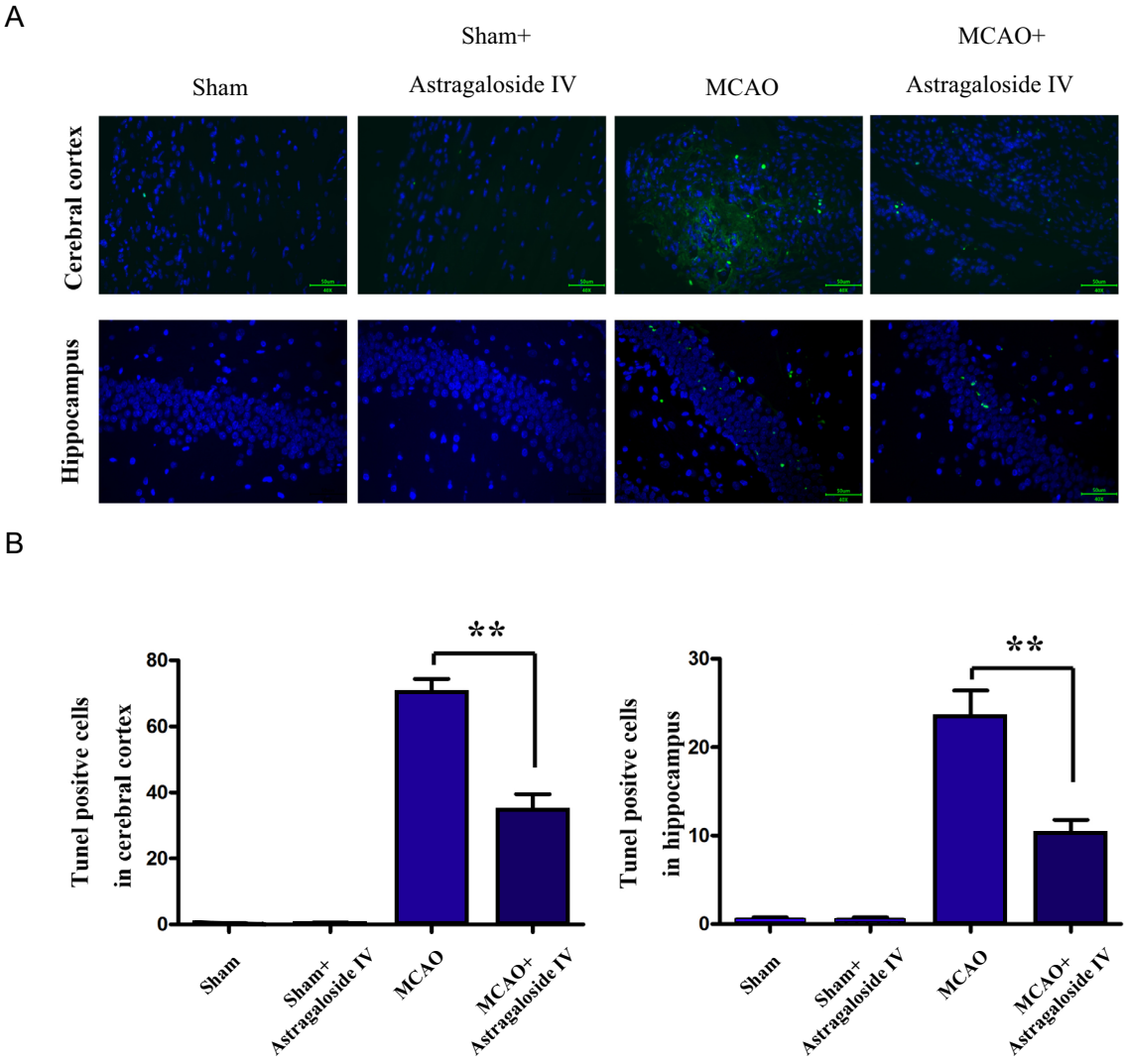

Figure. 2. Astragaloside IV inhibited CIRI-induced apoptosis in the hippocampus and cerebral cortex. The representative of TUNEL staining in the infarct area from four groups was shown (magnification: 40×; scale bar: 50 μm). The data are represented as the mean ± SEM. $^{**}P<0.01$, MCAO group versus MCAO+Astragaloside IV group, n = 8. The error bars represent the SEM. Statistical analysis was performed using an unpaired, two-tailed Student's t-test.

The therapeutic effects of Astragaloside IV on oxidative stress and mitochondrial calcium overload after CIRI

The protein levels related to mitochondrial calcium overload (Fig. 4A) and oxidative stress (Fig. 4B) were determined by a Western blot. The representative blots and bar graphs from four groups are displayed. β-actin was employed as the loading control. The columns represent the semi-quantified optidensity normalized by β-actin. The Western blot assay revealed that Astragaloside IV significantly decreased the protein levels associated with oxidative stress (p22, p47, GP91) and mitochondrial calcium overload (p-GRK2, p-PLCβ, p-PLCA, p-CaMKII, p-IP3R) in the brains of MCAO mice.

The therapeutic effects of Astragaloside IV on apoptosis after CIRI

The protein levels related to apoptosis were determined by Western blot. Representative blots (Fig. 5A) and bar graphs (Fig. 5B) from four groups are shown. β-actin was used as a loading control. The columns represent the semi-quantified optidensity, normalized by β-actin. The Western blot assay revealed that Astragaloside IV significantly inhibited the expression of pro-apoptotic proteins (cleaved caspase 3, cleaved caspase 8, cleaved caspase 9, Bax) while promoting the expression of the anti-apoptotic protein (Bcl-2) in the brains of MCAO mice.

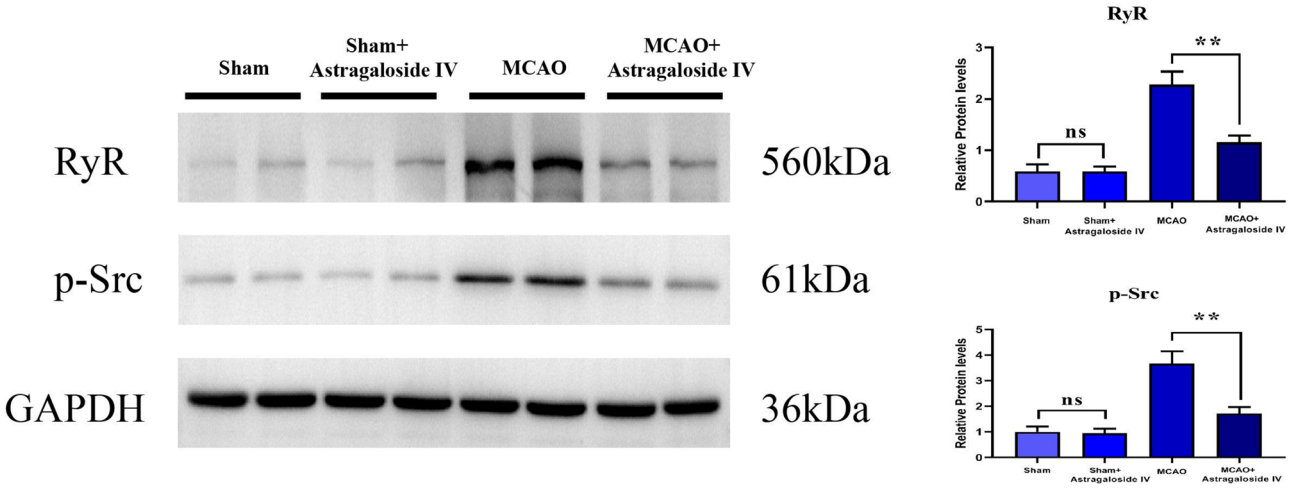

Figure. 3. Astragaloside IV inhibited the expression of RyR and p-Src in the MCAO mouse model. The protein levels of RyR and p-Src were detected by Western blot. Representative blots and bar graphs from four groups were shown. Images were cropped, and full-length blots were presented in Supplementary Fig. 3. The data are represented as the mean ± SEM. $^{**}P<0.01$, MCAO group vs. MCAO+Astragaloside IV group, ns means no statistical significance between the two groups, n = 8. The error bars represent the SEM. Statistical analysis was performed using an unpaired, two-tailed Student's t-test.

In vitro and *in vivo* experiments confirmed that Astragaloside IV attenuates oxidative stress in CIRI

The results of *in vivo* experiments demonstrated that the levels of ROS and MDA increased, while the level of SOD decreased in the brains of mice post-MCAO. However, Astragaloside IV significantly reduced the levels of ROS and MDA and elevated the expression of SOD (Fig. 6A). As depicted in Fig. 6B, the results of the cellular experiments agreed with the *in vivo* experiments, offering further evidence that Astragaloside IV may alleviate the oxidative stress caused by CIRI.

Astragaloside IV increased the viability and attenuated apoptosis of PC12 cells after OGD/R

The flow cytometry data revealed a significant increase in the apoptosis rate of PC12 cells after OGD/R. However, Astragaloside IV significantly lowered the apoptosis rate of OGD/R PC12 cells (Fig. 7A, B), indicating its apoptosis-inhibiting effect. The CCK-8 assay indicated a significant decrease in cell viability post OGD/R, but Astragaloside IV managed to enhance cell viability after OGD/R (Fig. 7C).

Astragaloside IV protected PC12 cells against apoptosis by inhibiting the p-GRK2 signaling pathway *in vitro*

The protein levels related to the p-GRK2 signaling pathway (Fig. 8A) and apoptosis (Fig. 8B) were determined by a Western blot. Representative blots and bar graphs from four groups are presented, with β-actin serving as a loading control. The columns represent the semi-quantified optidensity normalized by β-actin. The Western blot assay revealed that Astragaloside IV notably decreased the related protein levels of the p-GRK2 signaling pathway (p-GRK2, p-IP3R, p-PLCγ) and apoptosis (p22, p47, caspase 3, Bax) in the PC12 cells. Representative double immunofluorescence staining (Fig. 8C) for p-GRK2 and nuclei displayed the spatial distribution of p-GRK2 within the PC12 cells. GSK180736A is the most effective inhibitor of GRK2[39]. Astragaloside IV also has a comparably inhibitory effect, albeit to a lesser degree. Therefore, Astragaloside IV + GSK180736A was chosen in this study to achieve dual inhibition. The results showed that Astragaloside IV, GSK180736A, and Astragaloside IV + GSK180736A all reduced the fluorescence intensity of p-GRK2. The effect of Astragaloside IV + GSK180736A was better, although the difference was not significant (Fig. 8C).

Discussion

CIRI is a globally recognized public health problem that has gained significant attention in terms of its prevention and treatment. Investigating the molecular mechanism of CIRI is paramount for targeted drug research. Neuronal apoptosis is thought to be one of the foundational factors contributing to CIRI[5]. This study demonstrates that Astragaloside IV can thwart PC12 cell apoptosis after OGD/R by constraining the p-GRK2 signaling pathway *in vitro*. In MCAO mouse models, treatment with Astragaloside IV diminished oxidative stress and mitochondrial calcium overload following CIRI. Moreover, Astragaloside IV decreased CIRI-induced apoptosis in the hippocampus and cerebral cortex by reducing the expression of P-Src and P-GRK2 due to inhibited expression of RyR.

The efficacy of RyR as an intracellular Ca^{2+} release channel depends on strict regulation of gating and high rates of Ca^{2+} movement through open channels. RyR channels, located in the endo/sarcoplasmic reticulum (ER/SR) membrane, control the release of Ca^{2+} from intracellular repositories. Substantial Ca^{2+} flux from the ER/

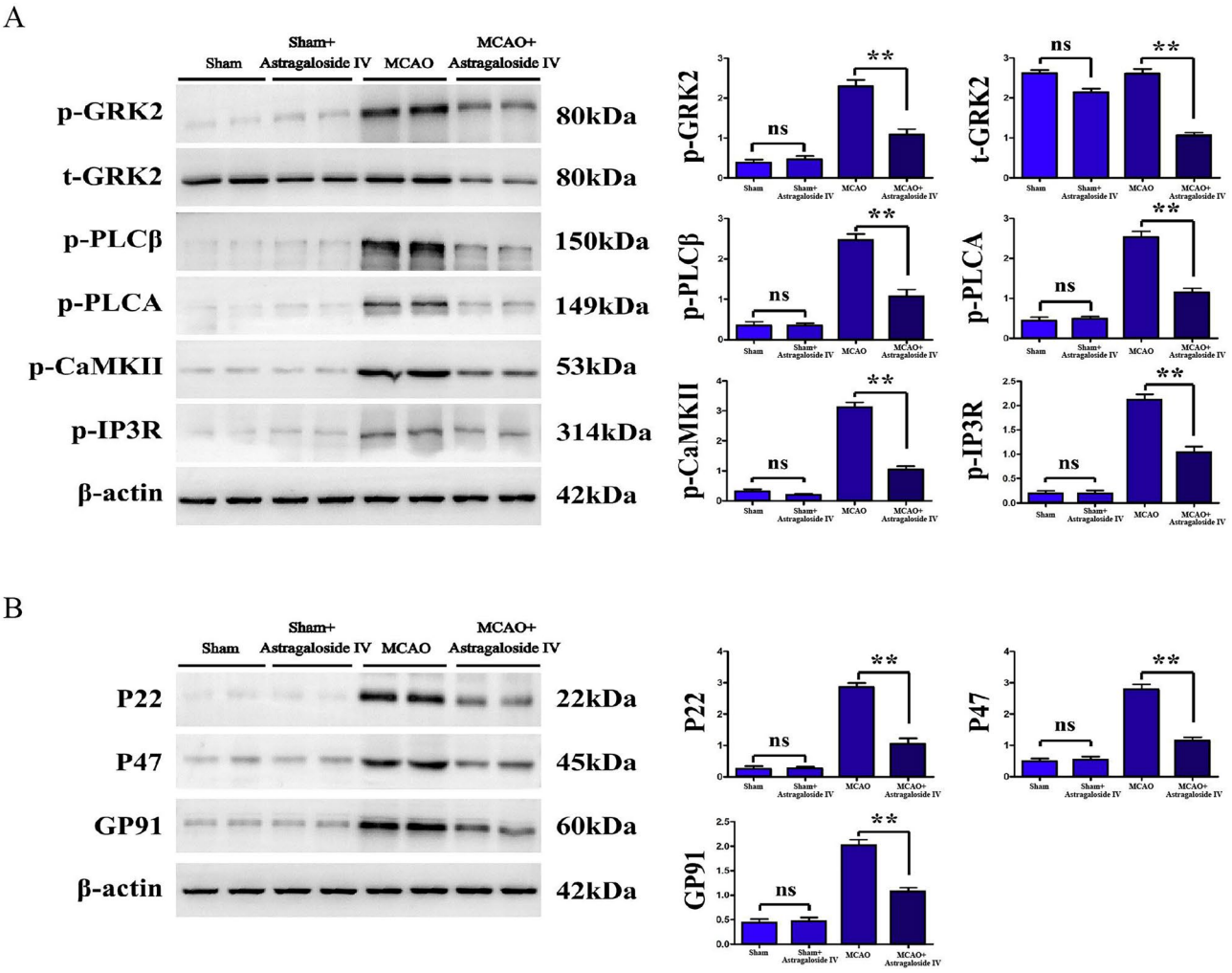

Figure. 4. The therapeutic effects of Astragaloside IV on oxidative stress and mitochondrial calcium overload after CIRI. The related protein levels of mitochondrial calcium overload (**A**) and oxidative stress (**B**) were determined by Western blot. Representative blots and bar graphs from four groups were shown. Images were cropped, and full-length blots are presented in Supplementary Fig. 4. The data are represented as the mean ± SEM. $^{**}P<0.01$, MCAO group vs. MCAO+Astragaloside IV group, ns means no statistical significance between the two groups, n = 8. The error bars represent the SEM. Statistical analysis was performed using an unpaired, two-tailed Student's t-test.

SR into the cytosol – through clusters of RyRs across the cell – ultimately leads to a global increase in intracellular Ca^{2+} concentration ($[Ca^{2+}]_i$). This increase results in muscle contraction, neuronal exocytosis, or apoptosis when Ca^{2+} levels meet an adequate threshold. Furthermore, RyR can influence or be influenced by Ca^{2+} signals instigated by other channels. Consequently, RyRs function as cell signaling integration centers, originating various types of Ca^{2+} signals[41].

The change in intracellular Ca^{2+} concentration functions as a key second messenger to initiate endogenous apoptosis. The release of intracellular Ca^{2+} is primarily mediated by IP3R and RyR on the sarcoplasmic reticulum plasma membrane. MCAO provokes brain cells into a state of hypoxia and hypoglycemia. Following hypoxia, the IP3R/RyR-mediated increase in intracellular Ca^{2+} concentration induces apoptosis. Within the mitochondrial apoptosis pathway, mitochondria perceive endogenous and external death pressures via various signal transduction modes. Crucial molecules like Ca^{2+} and Bcl-2 family proteins regulate this process, causing signal molecules, such as Cytochrome C (Cytc), to be released by altering mitochondrial membrane permeability. These molecules activate downstream caspase cascade reactions, initiating cell apoptosis. Consequently, changes in intracellular Ca^{2+} concentration play a significant role as the second messenger in cell apoptosis, and Ca^{2+} concentration regulation is strongly associated with the initiation of the mitochondrial apoptosis pathway. The sarcoplasmic reticulum serves as the most vital calcium reservoir in smooth muscle cells, with IP3R and RyR being the primary channels for Ca^{2+} release. Under hypoxic stimulation, IP3R and RyR channels are activated, leading to Ca^{2+} flowing out of the sarcoplasmic reticulum and increasing the concentration of Ca^{2+} in the cytoplasm. Hence, IP3R/RyR-mediated increases in intracellular calcium concentration are important signals for initiating the mitochondrial apoptosis pathway.

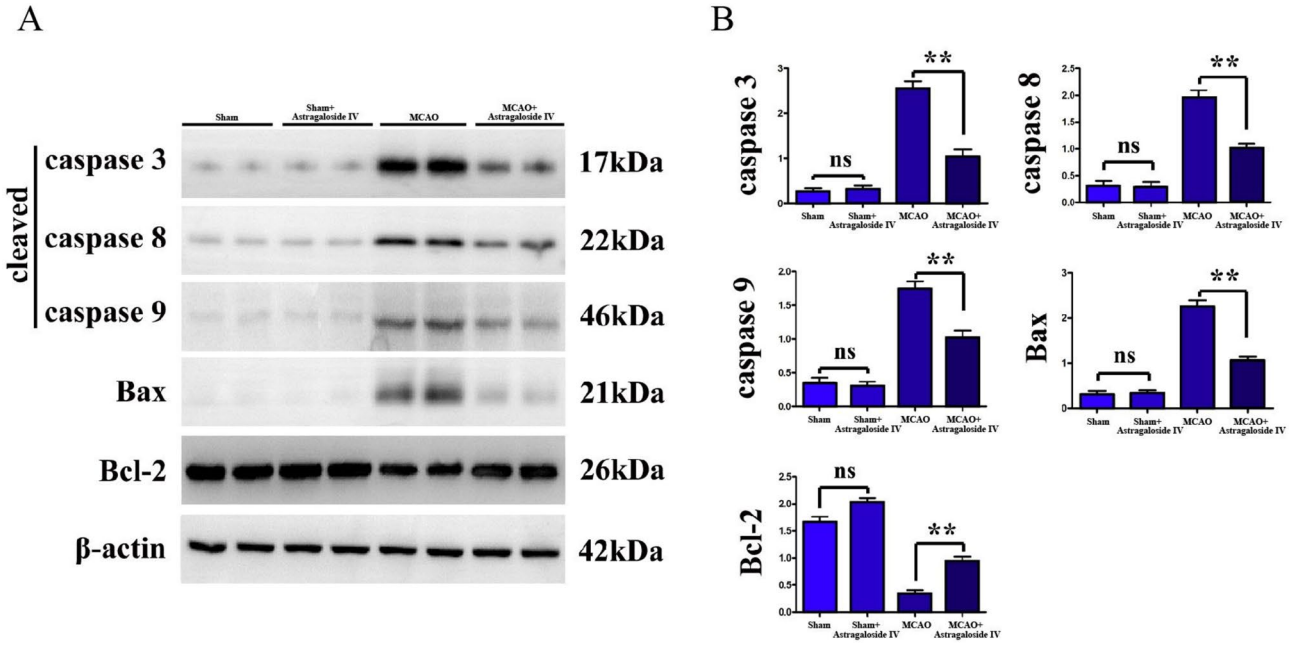

Figure. 5. The therapeutic effects of Astragaloside IV on apoptosis after CIRI. The related protein levels of apoptosis were determined by Western blot. Representative blots (**A**) and bar graphs (**B**) from four groups were shown. Images were cropped, and full-length blots are presented in Supplementary Fig. 5. The data are represented as the mean ± SEM. $^{**}P < 0.01$, MCAO group vs. MCAO+Astragaloside IV group, ns means no statistical significance between the two groups, n = 8. The error bars represent the SEM. Statistical analysis was performed using an unpaired, two-tailed Student's t-test.

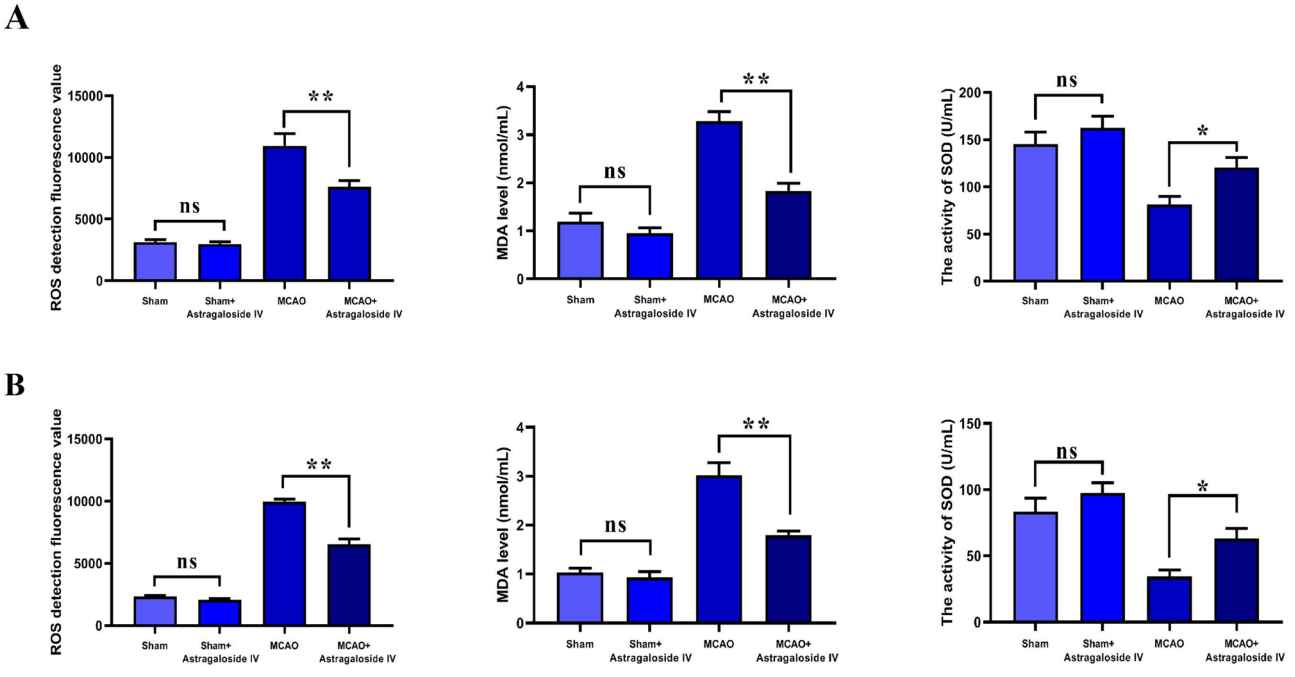

Figure. 6. The therapeutic effects of Astragaloside IV on oxidative stress. **A** Statistical results of ROS, MDA, and SOD in brain tissues of four groups of mice. **B** Statistical results of ROS, MDA, and SOD in four groups of PC12 cells. The data are represented as the mean ± SEM. $^{*}P < 0.05$, $^{**}P < 0.01$, MCAO group vs. MCAO+Astragaloside IV group, $^{*}P < 0.05$, $^{**}P < 0.01$, OGD/R group vs. OGD/R+Astragaloside IV group, ns means no statistical significance between the two groups, n = 8. The error bars represent the SEM.

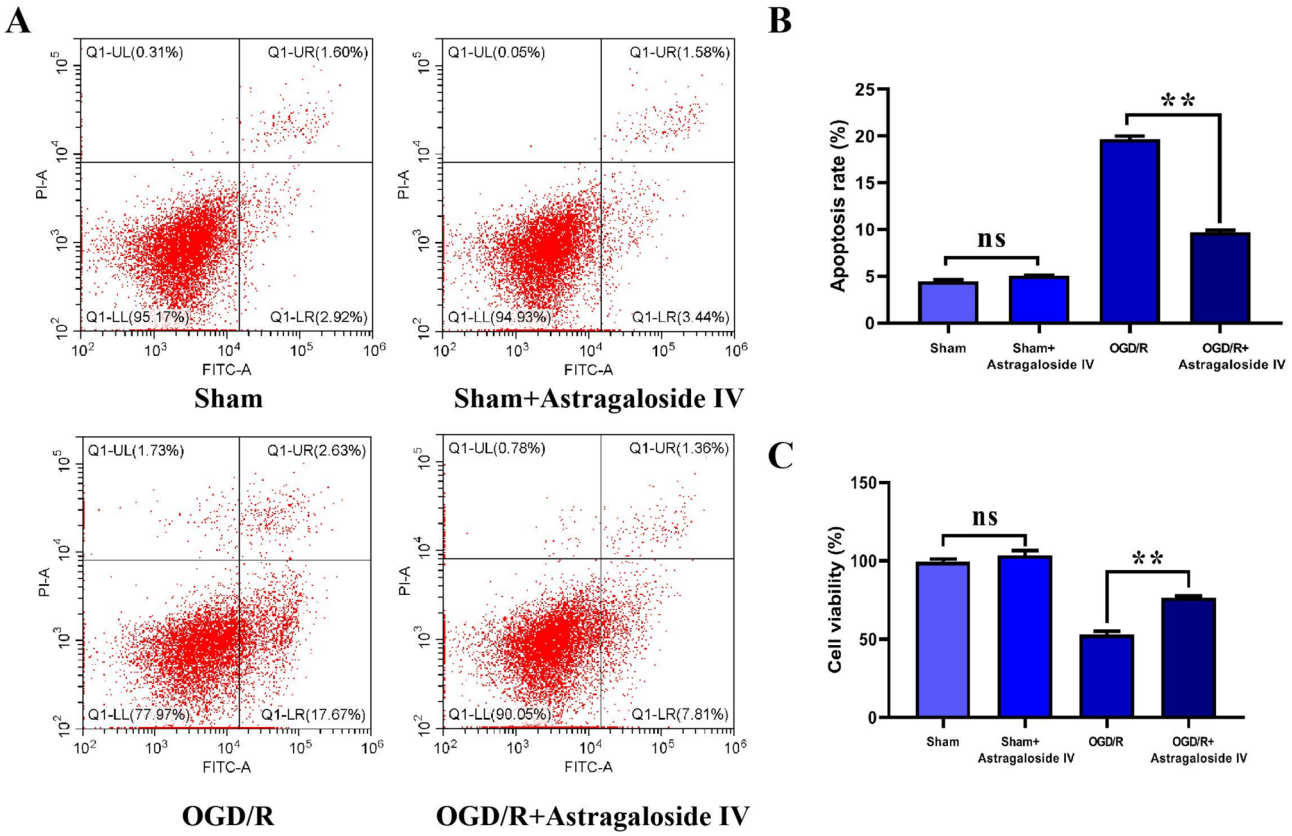

Figure. 7. The therapeutic effects of Astragaloside IV on cell viability and apoptosis. **A** Representative photographs were obtained from four groups. **B** Statistical results of apoptosis rate in four groups of PC12 cells. **C** Statistical results of cell viability in four groups. The data are represented as the mean ± SEM. $^{**}P < 0.01$, OGD/R group vs. OGD/R+Astragaloside IV group, ns means no statistical significance between the two groups, n = 8. The error bars represent the SEM.

Under the influence of a hypoxia signal, the G protein on the surface of the cell membrane is activated. Subsequently, this G protein activates the phospholipase C (PLC) in the cytoplasm. PLC then hydrolyzes 4,5-diphosphatidylinositol (PIP2) into inositol phosphate 3 (IP3) and diacylglycerol (DAG). IP3 is transported from the cytoplasm to the sarcoplasmic surface where it binds with IP3R. This binding opens the IP3R pore, leading to the release of Ca^{2+} in the sarcoplasmic reticulum and an increase in cytoplasmic Ca^{2+} concentration. Consequently, the G protein pathway under hypoxia stimulation can rapidly increase IP3R protein expression, but this is not solely determined by the transcription level of the IP3R/RyR gene[42].

Src plays a regulatory role in receptor-mediated signal transduction and cell communication[43,44]. It was discovered that anchoring of Src kinase enhances the Ca^{2+} sensitivity of RyR[45]. Furthermore, phosphorylation of Src kinase increases RyR's Ca^{2+} sensitivity. Src-mediated phosphorylation of GRK2 is also pivotal for the hydrolysis of the GRK2 protein[46]. Tyrosine kinase Src, another component of the pro-mitotic signaling pathway, also regulates the phosphorylation of GRK2. Overexpressing the persistently activated Src mutant results in the tyrosine phosphorylation of co-expressed GRK2, and this increases its activity towards receptor and non-receptor substrates. Studies propose a model of cross-regulation between the receptor tyrosine kinase and GPCR signaling pathway, signifying P42/P44 and Src as physiological regulators of GRK activity[47].

Apoptosis constitutes a crucial link in cerebral ischemia and plays a significant role. This form of neuronal death is prominent in various types of cerebral ischemia. Recent studies reveal that brain injury induced by hypoxia and ischemia can trigger an excessive release of excitatory neurotransmitters. This results in continuous depolarization of the postsynaptic membrane, causing a significant influx of calcium, which initiates a series of intracellular calcium biochemical reactions, leading to neuronal apoptosis[48,49]. The Ca^{2+} signaling pathway plays a critical role in cell survival, proliferation, and metabolism. The mechanism involves Ca^{2+} entering the cell and binding with Calmodulin (CaM) to form Ca^{2+}-CaM[50–52], which activates the Calmodulin-dependent protein kinase II (CaMKII). The phosphorylated CaMKII can directly trigger cAMP response element-binding protein (CREB), further regulating the synthesis of cytoskeleton protein and synaptic protein. Through phosphorylation, CREB can diminish neuronal apoptosis and advance neuronal formation by initiating downstream anti-apoptotic proteins[53,54].

Intracellular calcium disturbances lead to increased PLC-γ phosphorylation and IP3 production. Phospholipase C (PLC-γ) has two subclasses, specifically PLC-γ1 and PLC-γ2. Under normal conditions, these exist in the cytoplasm but can bind to the cell membrane after activation[55]. Various extracellular factors activate PLC-γ, which hydrolyzes PIP2, leading to two intracellular products: IP3 and DAG. The former induces the

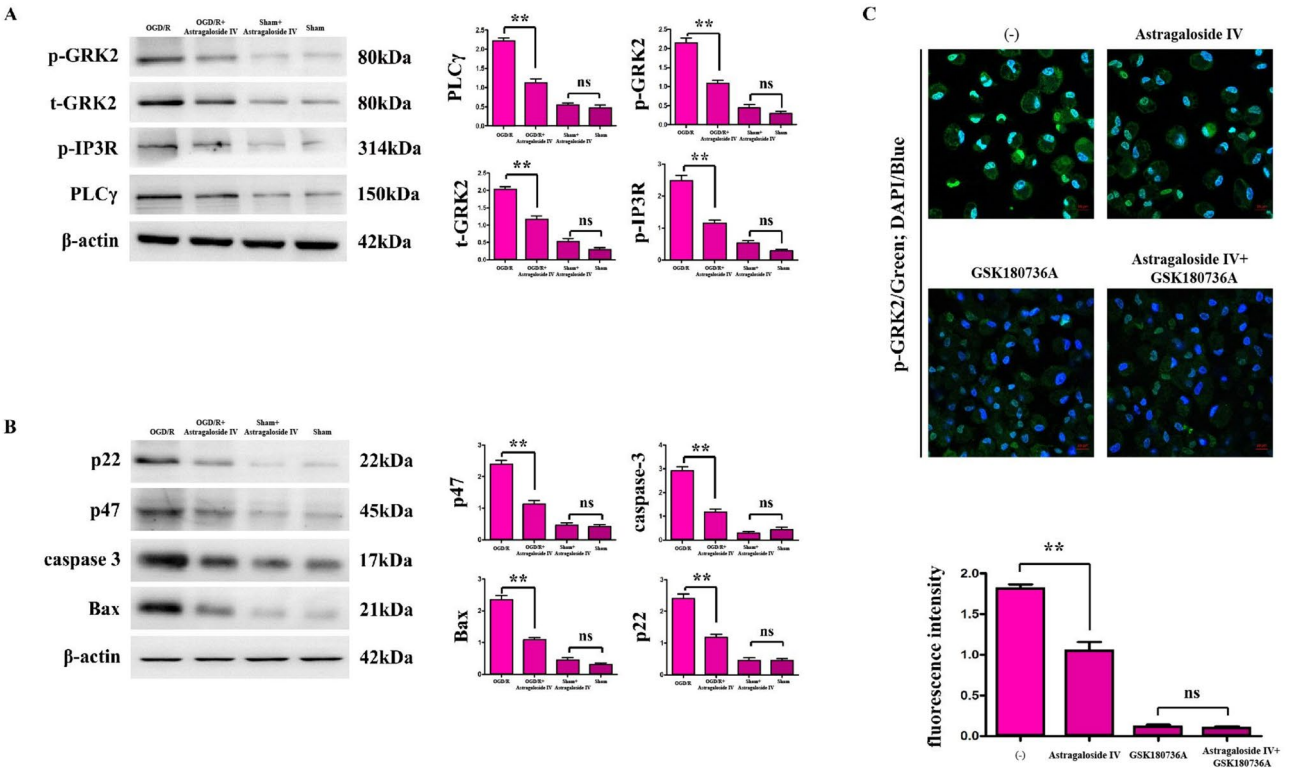

Figure. 8. Astragaloside IV protected PC12 cells against apoptosis by inhibiting the p-GRK2 signaling pathway *in vitro*. The related protein levels of p-GRK2 signaling pathway (**A**) and apoptosis (**B**) were determined by Western blot. Representative blots and bar graphs from four groups were shown. Images were cropped, and full-length blots were presented in Supplementary Fig. 8. **C** Representative double immunofluorescence staining. The data are represented as the mean ± SEM. $^{**}P < 0.01$, control group vs. Astragaloside IV group, ns means no statistical significance between the two groups. The error bars represent the SEM. Statistical analysis was performed using an unpaired, two-tailed Student's t-test.

release of intracellular calcium ions and activates the intracellular calcium signaling pathway. The latter acts on protein kinase C (PKC), triggering a series of biochemical reactions that regulate cell growth, differentiation, and apoptosis[42].

Under physiological conditions, Ca^{2+} is transported into the endoplasmic reticulum by SERCA and released into the cytoplasm by RyR and IP3R channels, thereby stabilizing the free Ca^{2+} in the endoplasmic reticulum. IP3, one of the products generated after the activation of PLC-γ, is a calcium regulatory signal. When it binds with IP3 receptors in the endoplasmic reticulum, it stimulates the release of calcium ions from the calcium pool in the endoplasmic reticulum, thus regulating the intracellular calcium signaling pathway[56,57]. In recent years, additional research on its function has confirmed that IP3 is an essential signal for the release of calcium ions from the endoplasmic reticulum and that PLC-γ is crucial for activating calcium ions to enter cells via plasma membrane channels[58–60].

During ischemia, the influx of extracellular Ca^{2+} leads to an increase in $[Ca^{2+}]_i$, which concurrently transfers to the mitochondria. This results in mitochondrial calcium ($[Ca^{2+}]$) overload, thereby activating a series of calcium-dependent proteases that amplify the accumulation of lipid peroxidation products and ROS. Post-reperfusion, the ischemic tissue receives an ample oxygen supply, which in turn activates xanthine oxidase; this generates a multitude of oxygen free radicals, triggers the lipid peroxidation reaction, and results in massive nerve cell necrosis and microcirculation disorders[61,62]. Energy depletion in cells induced by ischemia impacts the Ca^{2+}-Mg^{2+}-ATPase activity, thus leading to a decreased energy-dependent $[Ca^{2+}]$. The associated reduction in outward migration and decreased mitochondrial uptake of $[Ca^{2+}]_i$ extends glutamate receptor-mediated neuronal excitation, consequently causing neuronal death[63].

Astragalus saponins can enhance SOD activity, stifle the production of free radicals, and diminish the apoptosis of nerve cells in a rat model with CIRI. Research indicates that Astragalus injection can significantly curb hypoxia-induced apoptosis of nerve cells cultured *in vitro*, as detected by Hoechst 33342 staining. However, after 12 h of hypoxia, the inhibitory effect remains notably inferior to that of the positive apoptotic group—similar to the anti-apoptotic cytokine brain-derived neurotrophic factor (BDNF). Astragalus injection can directly boost the expression of Bcl-2 and reduce the expression of Bax in hypoxic nerve cells, thereby achieving an anti-apoptotic effect[64].

Astragaloside IV is one of the primary active ingredients found in *A. membranaceus*. It demonstrates many functions such as scavenging oxygen free radicals, battling inflammation and viruses, boosting immunity, and improving cardiovascular function[30]. Astragaloside IV can also decrease the activity of myeloperoxidase and

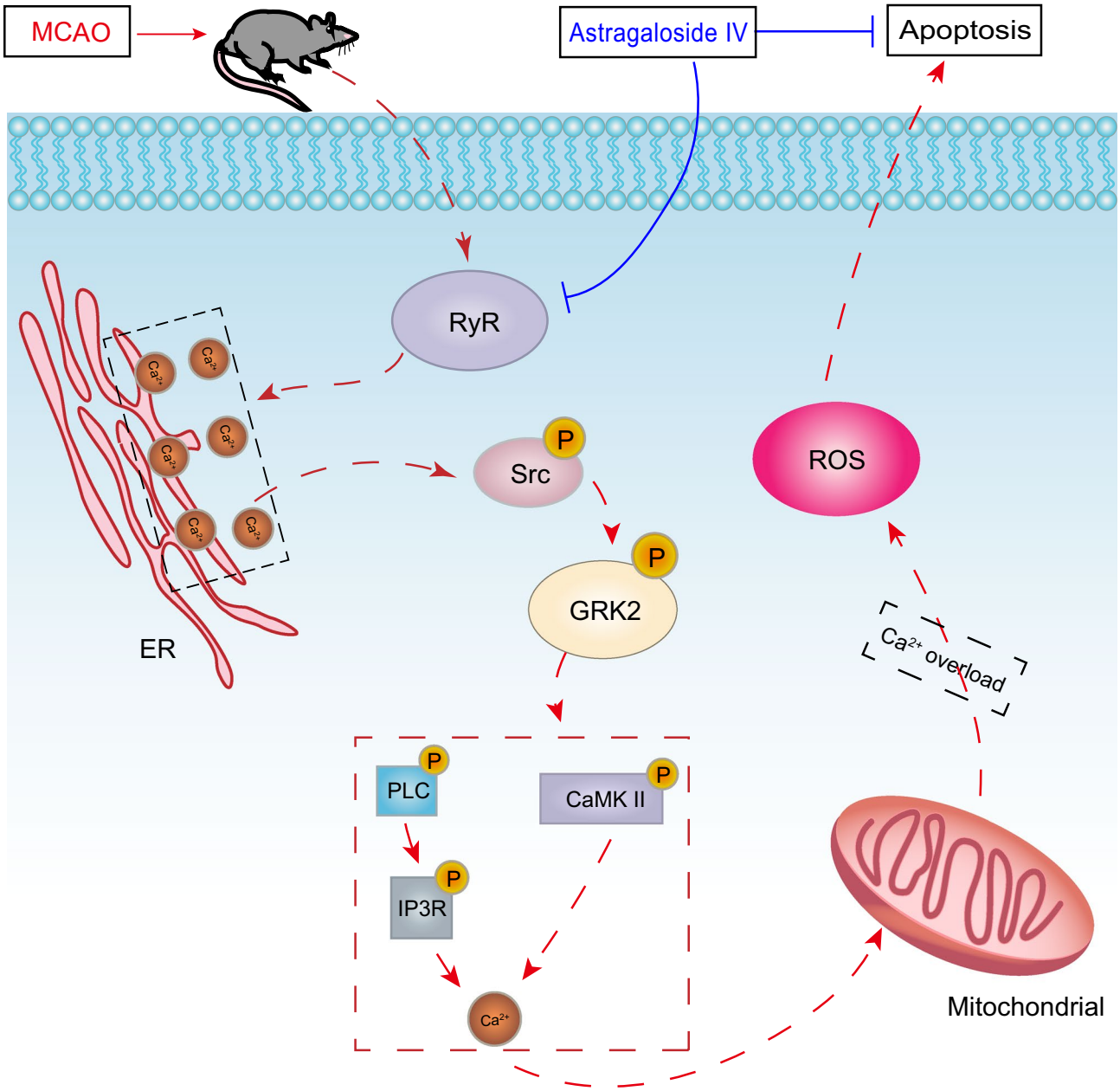

Figure. 9. Mechanism diagram of Astragaloside IV improving apoptosis following cerebral ischemia-reperfusion injury cells.

reduce inflammation in rats experiencing cerebral ischemia-reperfusion[65]. After treating PC12 cells with Astragaloside IV, both the apoptosis rate and apoptosis index underwent significant decreases[66,67]. In this study, Astragaloside IV was identified as alleviating oxidative stress, bolstering cell viability, and reducing apoptosis following CIRI. These findings align with our study's results. Although Astragaloside IV does not appear in Table 1, the current study's findings suggest that it is indeed an active ingredient in *A. membranaceus* with potential impacts on ischemic stroke.

The review indicates that Astragaloside IV potentially exerts a neuroprotective effect on cerebral ischemia/reperfusion injury largely through its antioxidant, anti-inflammatory, and anti-apoptotic properties[68]. This is partially based on previous publications about Astragaloside IV's mechanisms: it can inhibit apoptosis via the transforming growth factor-β1/Smad2 signaling pathway, reduce oxidative stress through the p38 MAPK pathway, downregulate the TLR4/NF-κB signaling pathway to lessen myocardial I/R injury in rats, and stimulate angiogenesis via the phosphatidylinositol 3-kinase/Akt pathway. Astragaloside IV could ease oxidative stress and suppress inflammatory stress and apoptosis in acute ischemic stroke animal models by regulating downstream signaling cascade molecules, proinflammatory mediators, inflammatory mediators, and the anti-apoptotic regulator. However, in this study, we found that Astragaloside IV could alleviate apoptosis after CIRI by reducing the expression of P-Src and P-GRK2, indirectly courtesy of inhibiting RyR expression and/or activation.

Conclusion

In summary, the key findings of this study indicate that MCAO induces a state of hypoxia and hypoglycemia in brain cells. This activates RyR, which in turn increases the release of Ca^{2+} from the endoplasmic reticulum. This upsurges the expression of phosphorylated Src, promoting the phosphorylation of GRK2, and triggering mitochondrial Ca^{2+} overload. The overloaded p-GRK2 instigates mitochondrial Ca^{2+} in two ways: ① By encouraging the amplification of CaMKII phosphorylation, Ca^{2+} is ushered into mitochondria; ② By bolstering the increment in PLC phosphorylation leading to the surge in phosphorylated IP3R, which allows Ca^{2+} to enter mitochondria. Overloading of mitochondrial Ca^{2+} can further excite ROS and usher in apoptosis of brain cells. However, Astragaloside IV can resist RyR expression and hence, mitigate apoptosis of brain cells (Fig. 9). Moreover, Astragaloside IV can directly keep brain cell apoptosis in check.

Data availability

The datasets generated and/or analyzed during the current study are available from the corresponding author upon reasonable request.

Received: 29 December 2022; Accepted: 24 July 2024
Published online: 30 July 2024

References

1. Michels, P. Acute treatment of cerebral infarction. *Fortschr. Neurol. Psychiatr.* **81**(3), 169–174. https://doi.org/10.1055/s-0032-1330347 (2013).
2. Tramacere, I. *et al.* Comparison of statins for secondary prevention in patients with ischemic stroke or transient ischemic attack: A systematic review and network meta-analysis. *BMC Med.* **17**(1), 67. https://doi.org/10.1186/s12916-019-1298-5 (2019).
3. Leiva-Salinas, C., Wintermark, M. & Kidwell, C. S. Neuroimaging of cerebral ischemia and infarction. *Neurotherapeutics.* **8**(1), 19–27. https://doi.org/10.1007/s13311-010-0004-2 (2011).
4. Mistry, E. *et al.* Mechanical thrombectomy outcomes with and without intravenous thrombolysis in stroke patients: A meta-analysis. *Stroke* **48**(9), 2450–2456. https://doi.org/10.1161/strokeaha.117.017320 (2017).
5. Li, H. *et al.* γ-Glutamylcysteine alleviates ischemic stroke-induced neuronal apoptosis by inhibiting ros-mediated endoplasmic reticulum stress. *Oxid. Med. Cell Longev.* **2021**, 2961079. https://doi.org/10.1155/2021/2961079 (2021).
6. Liu, X. *et al.* By targeting apoptosis facilitator bcl2l13, microrna mir-484 alleviates cerebral ischemia/reperfusion injury-induced neuronal apoptosis in mice. *Bioengineered* **12**(1), 948–959. https://doi.org/10.1080/21655979.2021.1898134 (2021).
7. Liu, X. *et al.* Knockdown of pvt1 exerts neuroprotective effects against ischemic stroke injury through regulation of mir-214/gpx1 axis. *Biomed. Res. Int.* **2022**, 1393177. https://doi.org/10.1155/2022/1393177 (2022).
8. Gao, H. *et al.* Ligustrazine monomer against cerebral ischemia/reperfusion injury. *Neural Regen. Res.* **10**(5), 832–840. https://doi.org/10.4103/1673-5374.156991 (2015).
9. Wang, Z. *et al.* Therapeutic potential of novel twin compounds containing tetramethylpyrazine and carnitine substructures in experimental ischemic stroke. *Oxid. Med. Cell Longev.* **2017**, 7191856. https://doi.org/10.1155/2017/7191856 (2017).
10. Luo, J. *et al.* 6-Gingerol protects against cerebral ischemia/reperfusion injury by inhibiting nlrp3 inflammasome and apoptosis via trpv1 / faf1 complex dissociation-mediated autophagy. *Int. Immunopharmacol.* **100**, 108146. https://doi.org/10.1016/j.intimp.2021.108146 (2021).
11. Kao, T. *et al.* Neuroprotection by tetramethylpyrazine against ischemic brain injury in rats. *Neurochem. Int.* **48**(3), 166–176. https://doi.org/10.1016/j.neuint.2005.10.008 (2006).
12. Chen, B. *et al.* Cofilin inhibition by limk1 reduces rod formation and cell apoptosis after ischemic stroke. *Neuroscience.* **444**, 64–75. https://doi.org/10.1016/j.neuroscience.2020.07.019 (2020).
13. Superti-Furga, G. & Courtneidge, S. A. Structure-function relationships in Src family and related protein tyrosine kinases. *Bioessays* **17**(4), 321–330 (1995).
14. Aleshin, A. & Finn, R. S. Src: A century of science brought to the clinic. *Neoplasia* **12**(8), 599–607 (2010).
15. Paul, R. *et al.* Src deficiency or blockade of src activity in mice provides cerebral protection following stroke. *Nat. Med.* **7**(2), 222–227. https://doi.org/10.1038/84675 (2001).
16. Islam, M. Oxidative stress and mitochondrial dysfunction-linked neurodegenerative disorders. *Neurol. Res.* **39**(1), 73–82. https://doi.org/10.1080/01616412.2016.1251711 (2017).
17. Chen, Z. *et al.* Extracellular atp-induced nuclear ca2+ transient is mediated by inositol 1,4,5-trisphosphate receptors in mouse pancreatic beta-cells. *Biochem. Biophys. Res. Commun.* **382**(2), 381–384. https://doi.org/10.1016/j.bbrc.2009.03.030 (2009).
18. Park, J., Lo, E. & Hayakawa, K. Endoplasmic reticulum interaction supports energy production and redox homeostasis in mitochondria released from astrocytes. *Transl. Stroke Res.* **12**(6), 1045–1054. https://doi.org/10.1007/s12975-021-00892-7 (2021).
19. Ovcjak, A. *et al.* Ryanodine receptor inhibitor dantrolene reduces hypoxic-ischemic brain injury in neonatal mice. *Exp. Neurol.* **351**, 113985. https://doi.org/10.1016/j.expneurol.2022.113985 (2022).
20. Gurevich, E. V., Gainetdinov, R. R. & Gurevich, V. V. G protein-coupled receptor kinases as regulators of dopamine receptor functions. *Pharmacol. Res.* https://doi.org/10.1016/j.phrs.2016.05.010 (2016).
21. Gao, T. *et al.* The protective effect of allicin on myocardial ischemia-reperfusion by inhibition of ca overload-induced cardiomyocyte apoptosis via the pi3k/grk2/plc-γ/ip3r signaling pathway. *Aging* **13**(15), 19643–19656. https://doi.org/10.18632/aging.203375 (2021).
22. Hohendanner, F., McCulloch, A., Blatter, L. & Michailova, A. Calcium and ip3 dynamics in cardiac myocytes: Experimental and computational perspectives and approaches. *Front. Pharmacol.* **5**, 35. https://doi.org/10.3389/fphar.2014.00035 (2014).
23. Zhao, H. *et al.* Endoplasmic reticulum stress/ca-calmodulin-dependent protein kinase/signal transducer and activator of transcription 3 pathway plays a role in the regulation of cellular zinc deficiency in myocardial ischemia/reperfusion injury. *Front. Physiol.* **12**, 736920. https://doi.org/10.3389/fphys.2021.736920 (2021).
24. Zhang, J. *et al.* Novel camkii-δ inhibitor hesperadin exerts dual functions to ameliorate cardiac ischemia/reperfusion injury and inhibit tumor growth. *Circulation* **145**(15), 1154–1168. https://doi.org/10.1161/circulationaha.121.055920 (2022).
25. Wang, H., Zhou, Q., Xu, M., Zhou, X. & Zheng, G. Astragaloside iv for experimental focal cerebral ischemia: Preclinical evidence and possible mechanisms. *Oxid. Med. Cell Longev.* **2017**, 8424326. https://doi.org/10.1155/2017/8424326 (2017).
26. Zhao, X. *et al.* Inhibition of oxidative stress: an important molecular mechanism of chinese herbal medicine (astragalus membranaceus, carthamus tinctorius l., radix salvia miltiorrhizae, etc.) in the treatment of ischemic stroke by regulating the antioxidant system. *Oxid. Med. Cell Longev.* **2022**, 1425369. https://doi.org/10.1155/2022/1425369 (2022).
27. Du, S. *et al.* Astragaloside iv attenuates cerebral ischemia-reperfusion injury in rats through the inhibition of calcium-sensing receptor-mediated apoptosis. *Int. J. Mol. Med.* **47**(1), 302–314. https://doi.org/10.3892/ijmm.2020.4777 (2021).

28. Zhang, Y. *et al.* The role of astragaloside iv against cerebral ischemia/reperfusion injury: Suppression of apoptosis via promotion of p62-lc3-autophagy. *Molecules* https://doi.org/10.3390/molecules24091838 (2019).
29. Zhang, J., Wu, C., Gao, L., Du, G. & Qin, X. Astragaloside IV derived from astragalus membranaceus: A research review on the pharmacological effects. *Adv. Pharmacol.* **87**, 89–112. https://doi.org/10.1016/bs.apha.2019.08.002 (2020).
30. Yang, H. *et al.* Shengmai injection attenuates the cerebral ischemia/reperfusion induced autophagy via modulation of the AMPK, mTOR and JNK pathways. *Pharm. Biol.* **54**(10), 2288–2297. https://doi.org/10.3109/13880209.2016.1155625 (2016).
31. Li, M. *et al.* Astragaloside IV protects against focal cerebral ischemia/reperfusion injury correlating to suppression of neutrophils adhesion-related molecules. *Neurochem. Int.* **60**(5), 458–465. https://doi.org/10.1016/j.neuint.2012.01.026 (2012).
32. Du, S.-J. *et al.* Astragaloside IV attenuates cerebral ischemia-reperfusion injury in rats through the inhibition of calcium-sensing receptor-mediated apoptosis. *Int. J. Mol. Med.* **47**(1), 302–314. https://doi.org/10.3892/ijmm.2020.4777 (2021).
33. Yan, W. *et al.* Autophagy activation is involved in neuroprotection induced by hyperbaric oxygen preconditioning against focal cerebral ischemia in rats. *Brain Res.* **1402**, 109–121. https://doi.org/10.1016/j.brainres.2011.05.049 (2011).
34. Kerneis, M. *et al.* Platelet effect of prasugrel and ticagrelor in patients with ST-segment elevation myocardial infarction. *Arch. Cardiovasc. Dis.* **108**(10), 502–510. https://doi.org/10.1016/j.acvd.2015.04.004 (2015).
35. Zhang, S. *et al.* Dipeptidyl peptidase-4 inhibition prevents lung injury in mice under chronic stress via the modulation of oxidative stress and inflammation. *Exp. Anim.* **70**(4), 541–552. https://doi.org/10.1538/expanim.21-0067 (2021).
36. Break, M. *et al.* Cytotoxic activity of Boesenbergia rotunda extracts against nasopharyngeal carcinoma cells (HK1). cardamonin, a Boesenbergia rotunda constituent, inhibits growth and migration of HK1 cells by inducing caspase-dependent apoptosis and G2/M-phase arrest. *Nutr. Cancer* **73**(3), 473–483. https://doi.org/10.1080/01635581.2020.1751217 (2021).
37. Longa, E. Z., Weinstein, P. R., Carlson, S. & Cummins, R. Reversible middle cerebral artery occlusion without craniectomy in rats. *Stroke* **20**(1), 84–91 (1989).
38. Han, B. *et al.* Novel insight into circular rna hectd1 in astrocyte activation via autophagy by targeting mir142-tiparp: Implications for cerebral ischemic stroke. *Autophagy* **14**(7), 1164–1184. https://doi.org/10.1080/15548627.2018.1458173 (2018).
39. Homan, K. T. *et al.* Identification and structure-function analysis of subfamily selective g protein-coupled receptor kinase inhibitors. *ACS Chem. Biol.* **10**(1), 310–319. https://doi.org/10.1021/cb5006323 (2015).
40. Bouley, R. *et al.* Structural determinants influencing the potency and selectivity of indazole-paroxetine hybrid g protein-coupled receptor kinase 2 inhibitors. *Mol. Pharmacol.* **92**(6), 707–717. https://doi.org/10.1124/mol.117.110130 (2017).
41. Viero, C. *et al.* Techniques and methodologies to study the ryanodine receptor at the molecular, subcellular and cellular level. *Adv. Exp. Med. Biol.* **740**, 183–215. https://doi.org/10.1007/978-94-007-2888-2_8 (2012).
42. Kadamur, G. & Ross, E. M. Mammalian phospholipase c. *Annu. Rev. Physiol.* **75**, 127–154. https://doi.org/10.1146/annurev-physiol-030212-183750 (2013).
43. Chen, L. *et al.* Adipose-derived stem cells promote diabetic wound healing via the recruitment and differentiation of endothelial progenitor cells into endothelial cells mediated by the VEGF-PLCγ-ERK pathway. *Arch. Biochem. Biophys.* **692**, 108531. https://doi.org/10.1016/j.abb.2020.108531 (2020).
44. Han, R. & Bakker, A. J. The effect of the PKC inhibitor calphostin C and the PKC agonist phorbol 12-myristate 13-acetate on regulation of cytosolic Ca(2+) in mammalian skeletal muscle cells. *Toxicol. Appl. Pharmacol.* **212**(3), 247–255 (2006).
45. Plotkin, J. L. *et al.* Regulation of dendritic calcium release in striatal spiny projection neurons. *J. Neurophysiol.* **110**(10), 2325–2336. https://doi.org/10.1152/jn.00422.2013 (2013).
46. Penela, P., Elorza, A., Sarnago, S. & Mayor, F. Beta-arrestin- and c-Src-dependent degradation of G-protein-coupled receptor kinase 2. *EMBO J.* **20**(18), 5129–5138 (2001).
47. Mohammed, S. G., Ibrahim, I. A. A. E. H., Mahmoud, M. F. & Mahmoud, A. A. A. Carvedilol protects against hepatic ischemia/reperfusion injury in high-fructose/high-fat diet-fed mice: Role of g protein-coupled receptor kinase 2 and 5. *Toxicol. Appl. Pharmacol.* **382**, 14750. https://doi.org/10.1016/j.taap.2019.114750 (2019).
48. Hurtado, O. *et al.* Neuroprotection afforded by prior citicoline administration in experimental brain ischemia: Effects on glutamate transport. *Neurobiol. Dis.* **18**(2), 336–345 (2005).
49. Arranz, A. M., Gottlieb, M., Pérez-Cerdá, F. & Matute, C. Increased expression of glutamate transporters in subcortical white matter after transient focal cerebral ischemia. *Neurobiol. Dis.* **37**(1), 156–165. https://doi.org/10.1016/j.nbd.2009.09.019 (2010).
50. Nakka, V. P., Gusain, A., Mehta, S. L. & Raghubir, R. Molecular mechanisms of apoptosis in cerebral ischemia: Multiple neuroprotective opportunities. *Mol. Neurobiol.* **37**(1), 7–38 (2008).
51. Huang, J. *et al.* Gua lou gui zhi decoction exerts neuroprotective effects on post-stroke spasticity via the modulation of glutamate levels and ampa receptor expression. *Int. J. Mol. Med.* **31**(4), 841–848. https://doi.org/10.3892/ijmm.2013.1262 (2013).
52. Li, Y. *et al.* Ozone (O3) elicits neurotoxicity in spinal cord neurons (scns) by inducing er Ca(2+) release and activating the CAMKII/MAPK signaling pathway. *Toxicol. Appl. Pharmacol.* **280**(3), 493–501. https://doi.org/10.1016/j.taap.2014.08.024 (2014).
53. Calvo, M., Villalobos, C. & Núñez, L. Calcium imaging in neuron cell death. *Methods Mol. Biol.* **1254**, 73–85. https://doi.org/10.1007/978-1-4939-2152-2_6 (2015).
54. Mehta, S. L., Manhas, N. & Raghubir, R. Molecular targets in cerebral ischemia for developing novel therapeutics. *Brain Res. Rev.* **54**(1), 34–66 (2007).
55. Wing, M. R., Bourdon, D. M. & Harden, T. K. PLC-epsilon: A shared effector protein in Ras-, Rho-, and G alpha beta gamma-mediated signaling. *Mol. Interv.* **3**(5), 273–280 (2003).
56. Rhee, S. G. & Choi, K. D. Regulation of inositol phospholipid-specific phospholipase C isozymes. *J. Biol. Chem.* **267**(18), 12393–12396 (1992).
57. Leal, G., Comprido, D. & Duarte, C. B. BDNF-induced local protein synthesis and synaptic plasticity. *Neuropharmacology* **76**(Pt C), 639–656. https://doi.org/10.1016/j.neuropharm.2013.04.005 (2014).
58. Falasca, M. *et al.* Activation of phospholipase C gamma by PI 3-kinase-induced PH domain-mediated membrane targeting. *EMBO J.* **17**(2), 414–422 (1998).
59. Irfan, M., Kim, M. & Rhee, M. H. Anti-platelet role of korean ginseng and ginsenosides in cardiovascular diseases. *J. Ginseng. Res.* **44**(1), 24–32. https://doi.org/10.1016/j.jgr.2019.05.005 (2020).
60. Jijón-Lorenzo, R. *et al.* Presynaptic dopamine D2 receptors modulate [h]GABA release at striatopallidal terminals via activation of PLC → IP3 → calcineurin and inhibition of AC → cAMP → PKA signaling cascades. *Neuroscience* **372**, 74–86. https://doi.org/10.1016/j.neuroscience.2017.12.041 (2018).
61. Deluga, K. S., Plötz, F. B. & Betz, A. L. Effect of indomethacin on edema following single and repetitive cerebral ischemia in the gerbil. *Stroke* **22**(10), 1259–1264 (1991).
62. Yager, J. Y., Brucklacher, R. M. & Vannucci, R. C. Cerebral energy metabolism during hypoxia-ischemia and early recovery in immature rats. *Am. J. Physiol.* **262**(3 Pt 2), H672–H677 (1992).
63. Nishizawa, Y. Glutamate release and neuronal damage in ischemia. *Life Sci.* **69**(4), 369–381 (2001).
64. Linnik, M. D., Zahos, P., Geschwind, M. D. & Federoff, H. J. Expression of bcl-2 from a defective herpes simplex virus-1 vector limits neuronal death in focal cerebral ischemia. *Stroke* **26**(9), 1670–1674 (1995).
65. Kang, Z., Xiao, Q., Wang, L., Xiao, L. & Tang, B. The combination of astragaloside IV and *Panax notoginseng* saponins attenuates cerebral ischaemia-reperfusion injury in rats through ferroptosis and inflammation inhibition via activating Nrf2. *J Pharm Pharmacol.* **75**(5), 666–676. https://doi.org/10.1093/jpp/rgad011 (2023).

66. Liu, X. *et al.* Preliminary study on the anti-apoptotic mechanism of astragaloside IV on radiation-induced brain cells. *Int. J. Immunopathol. Pharmacol.* **34**, 2058738420954594. https://doi.org/10.1177/2058738420954594 (2020).
67. Huang, X.-P., Liu, X.-D. & Deng, C.-Q. Effects of the combination of active component extracts from *Astragalus membranaceus* and *Panax notoginseng* on apoptosis, reactive oxygen species and mitochondrial membrane potential of PC12 cells with oxidative injury. *Zhong Xi Yi Jie He Xue Bao = Journal of Chinese Integrative Medicine* **10**(10), 1127–1134 (2012).
68. Wang, H.-L., Zhou, Q.-H., Xu, M.-B., Zhou, X.-L. & Zheng, G.-Q. Astragaloside IV for experimental focal cerebral ischemia: Preclinical evidence and possible mechanisms. *Oxid. Med. Cell Longev.* **2017**, 8424326. https://doi.org/10.1155/2017/8424326 (2017).

Author contributions

Juan Chen and Jun Bao performed the study and wrote the manuscript. Xiujuan Jiang: Investigation. Wentao Yu: Data curation. Yunpeng Han: Validation. Xia Zhang: Supervision. Ying Zhang: Resources, Funding acquisition, Project administration. Guoxing Deng: Conceptualization, Methodology.

Funding

This study was supported by research grants from the National Natural Science Foundation of China general Project (No. 81873035), Scientific Research Project of Hebei Administration of Traditional Chinese Medicine (No. 2019070), Science and Technology Ability Improvement Project of Hebei University of Chinese Medicine (No. KTY2019050).

Competing interest

The authors declare no competing interests.

Additional information

Supplementary Information The online version contains supplementary material available at https://doi.org/10.1038/s41598-024-68462-z.

Correspondence and requests for materials should be addressed to Y.Z. or G.D.